# Numerical Examples of Compact Constant Mean Curvature Surfaces

Karsten Große-Brauckmann  Konrad Polthier

December 15, 1994, revised April 10, 1995

**Abstract**

We construct new examples of compact constant mean curvature surfaces numerically. A conjugate surface method allows to explicitly construct examples. We employ the numerical algorithm of Oberknapp and Polthier based on discrete techniques to find area minimizers in the sphere $\mathsf{S}^3$ and to conjugate them to surfaces of constant mean curvature in $\mathbb{R}^3$. We compute examples of genus 5 and 30 and discuss a further example of genus 3.

## Contents

# 1 Introduction

For a long time the sphere was the only known compact immersed surface of constant mean curvature 1 (MC1). By the result of Alexandrov there is no other embedded compact MC1 surface and by a theorem of Hopf the only way to immerse the sphere with MC1 is the round sphere. Nevertheless Wente discovered MC1 tori in 1986 [W] (see Figure 2 and 3) and his work became the starting point for an intensive study of MC1 surfaces.

Pinkall and Sterling classified all tori [PS] by the genus of a hyperelliptic Riemann surface. This genus should not be confused with the genus of the MC1 surface, which is of course 1 for a torus. Bobenko then found explicit formulas in terms of theta functions associated to the hyperelliptic Riemann surface [Bo, Thm.6.1]. The two papers actually consider a larger class of MC1 surfaces containing the tori. This class gives rise to a period problem for the subset of tori. Algebraic conditions for the solvability of the period problem were stated in [Bo], and Ercolani, Knörrer, Trubowitz [EKT] (also Jaggi [J]) proved that for each genus there are hyperelliptic curves such that these conditions are satisfied. Hence there are MC1 tori for every hyperelliptic genus. Heil implemented Bobenko's formulas and can solve the period problem numerically [H].

Kapouleas constructed compact MC1 surfaces of every genus greater than two by an implicit function argument [Kp1]. Each surface is based on a graph such that the vertices relate to spheres and the edges to pieces of Delaunay surfaces. Provided the graph is balanced, Kapouleas proves there exists a surface for a suitable scaling of the graph. This means that the edges contain a possibly large number of Delaunay 'bubbles'; furthermore the Delaunay handles must be thin. Since the number of bubbles as well as the thinness of the handles are the result of delicate estimates it is almost impossible to decide for a given surface whether it can be obtained by Kapouleas' method. This situation is somewhat similar to the tori for which it seems that the period problem is more likely to be solvable when the surfaces are larger. On the other hand, once the handle size and Delaunay piece length are known Kapouleas' surfaces are very explicit in that they are close to the union of the Delaunay pieces. In [Kp2] Kapouleas manages to glue $g \in \mathbb{N}$ Wente tori together at a single lobe. This yields compact MC1 surfaces of every genus, in particular the up to then open genus 2 case. The handles used are fundamentally different from those of the Delaunay-like surfaces. Kapouleas' Wente-like surfaces fuse tori with a large number of lobes; again the number is practically unknown.

For the first time a conjugate surface method was used by Lawson 1970 [L] to

prove existence of MC1 surfaces and later extended by Karcher [Ka] and one of the authors [G]. They constructed a number of periodic MC1 surfaces and surfaces with ends, as well as the Wente torus [G]. The conjugate surface method is more explicit than Kapouleas' method and works for sufficiently symmetric surfaces.

In the present work we use this method to construct numerically new compact MC1 surfaces of higher genus. As candidates we take highly symmetric MC1 surfaces 'close' to a collection of spheres which are joint by small handles. Existence of the Penta surface of genus 5 and the surface with icosahedral symmetry of genus 30 is discussed in detail, while the numerics could not decide an example of genus 3. With any of the methods mentioned before a hard problem is to solve the period problem. In simpler cases it can be settled by an intermediate value theorem [Ka] using a graph property, or by a degree argument [G]. Here we use the numerical algorithm of Oberknapp and Polthier [O] [OP] to deal with the period problem in more involved situations. The algorithm uses discrete techniques generalizing an algorithm of Pinkall and Polthier [PP] for minimal surfaces.

At first we review in Section 2 the conjugate surface construction for MC1 surfaces, in its standard $C^2$ description as well as in the $C^1$ form that is used for the numerical algorithm. We also explain the period problem that makes our examples unique (or isolated) for fixed symmetries. We then review the underlying discrete numerical algorithm in Section 3. In Section 4 we discuss a class of possible candidates, for which the necessary conditions of stability and balancing are satisfied. Three specific examples and their numerics are described in Section 5 in greater detail. In a future paper we want to explore further examples [GP].

The algorithms and the graphics were implemented using the mathematical programming environment Grape developed at the Sonderforschungsbereich 256 at the University of Bonn. Grape can be obtained on request via the second author.

# 2 The conjugate surface construction

We illustrate the main ideas of this method. For details see [G].

It is helpful to explain the conjugate surface construction for minimal surfaces in $\mathbb{R}^3$ first. Let $F$ be an immersion with normal $N$, metric $g(v,w) = dF(v) \cdot dF(w)$ and Weingarten map $A$ given by $g(Av,w) = dN(v) \cdot dF(w)$. A surface is determined by its metric $g$ and Weingarten map $A$ provided the integrability conditions, the equations of Gauß and Codazzi, are satisfied.

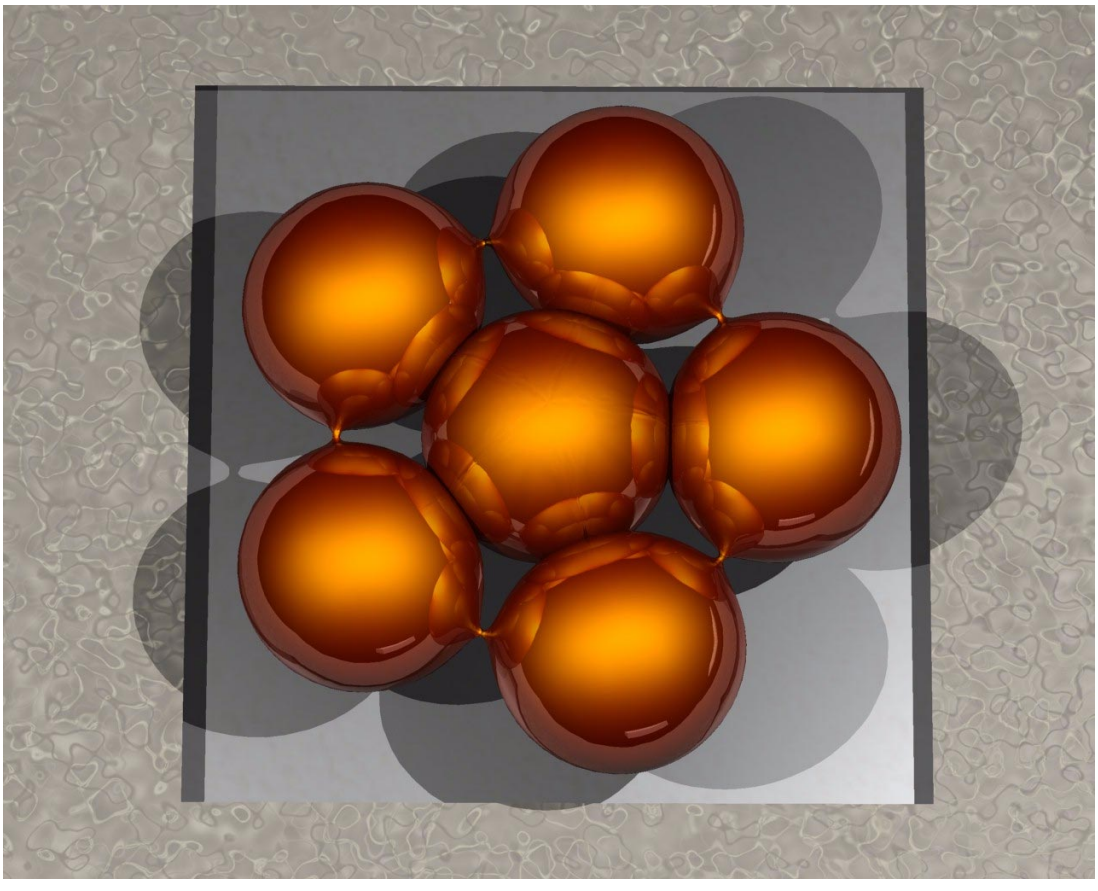

Figure 1: Surface Penta of genus 5. Small unduloidal handles connect the five outer spheres which, in turn, are joint to a centre sphere with nodoidal handles.

For a simply connected piece of an oriented minimal surface $M$ there is another surface $\tilde{M}$, the *conjugate surface*, with geometric data $\tilde{g}, \tilde{A}$ given by

$$\tilde{g} = g \quad \text{and} \quad \tilde{A} = R^{\pi/2} \circ A, \tag{1}$$

where $R^{\pm\pi/2}$ denotes rotation by $\pm\pi/2$ with respect to the metric $g$. The integrability conditions for $M$ can be checked to imply those of $\tilde{M}$.

Suppose we have an idea for the shape of a minimal surface with planar symmetries, and the surface modulo its symmetries gives a simply connected compact *fundamental patch*. To prove existence of such a patch via the conjugate surface construction it is essential that conjugation interchanges curvature and asymptote lines, and that geodesics are preserved. This is useful since the fundamental patch is bounded by planar, i.e. geodesic curvature lines, and hence relates to a conjugate patch bounded by geodesic asymptote lines. These lines are geodesics of the ambient space $\mathbb{R}^3$, i.e. straight lines, and therefore the conjugate patch

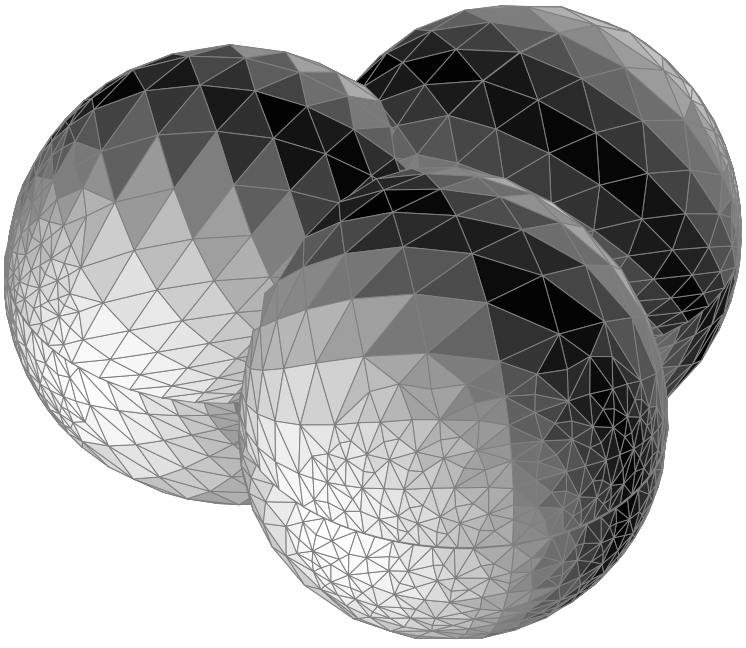

Figure 2: Wente torus with three lobes

is bounded by a polygon which has only finitely many parameters. We prove the claimed property in case $F(x)$ is a conformal curvature line parameterization of $\tilde{M}$. Let us write $A$ in matrix form, $A\frac{\partial}{\partial x_i} = A_i^j \frac{\partial}{\partial x_j}$. According to (1)

$$(2)\quad \tilde{A} = \begin{pmatrix} -\kappa & 0 \\ 0 & \kappa \end{pmatrix} \quad \text{and} \quad A = R^{-\pi/2}\tilde{A} = \begin{pmatrix} 0 & 1 \\ -1 & 0 \end{pmatrix}\begin{pmatrix} -\kappa & 0 \\ 0 & \kappa \end{pmatrix} = \begin{pmatrix} 0 & \kappa \\ \kappa & 0 \end{pmatrix}$$

i.e. the parametrization of $M$ is in asymptote lines.

We now want to determine the polygon on $M$ from the fundamental patch on $\tilde{M}$. Let the polygon on $\tilde{M}$ be bounded by $n$ planar curvature arcs $\tilde{\gamma}_i$. Then the conjugate arcs make the same angles at the vertices on the isometric surface $M$. Moreover, by definition of $A$ we obtain quantitative information from (2): The turning speed $-\kappa$ of the normal along the planar curvature line $\tilde{\gamma}_i$ on $\tilde{M}$ equals the rotation speed $\kappa$ of the normal along the straight line $\gamma_i$ of $M$. In particular, by an integration of (2) the total turn $\tilde{\tau}_i$ of the normal along the planar curvature line $\tilde{\gamma}_i$ equals the total rotation $\rho_i$ of the normal along the straight arc $\gamma_i$,

$$-\tilde{\tau}_i = \rho_i.$$

A closed polygon of straight arcs on $M$ is not completely determined by the $n$ vertex angles and the $n$ total rotations $\rho_i$ (up to euclidean motions and scaling); in general we are free to specify $n-3$ lengths of the polygon. For a given patch

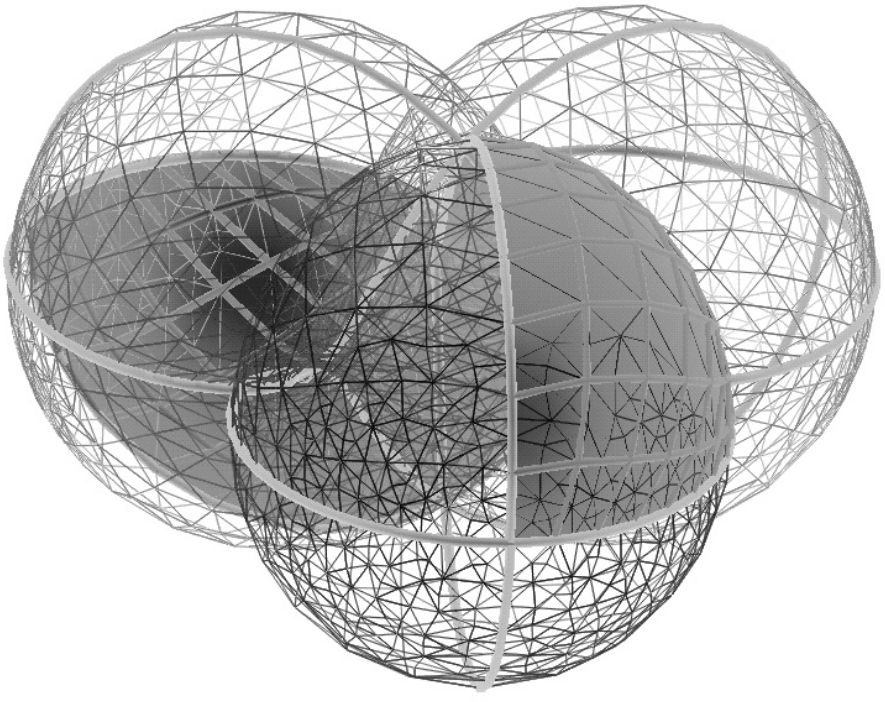

Figure 3: A grid model of the same Wente torus. A fundamental domain that generates the surface by planar reflection is highlighted.

bounded by planar symmetry curves this gives an $n-3$ parameter family of closed polygonal candidates. Hence by taking solutions to Plateau's problem for each closed polygon we get an $n-3$ parameter family of minimal patches $M$. Each conjugate patch $\tilde{M}$ can be reflected by the assumed group of planar symmetries to a complete branched immersed surface.

Lawson generalized this approach to CMC surfaces [L]. He found a one to one correspondence between MC1 surfaces in $\mathbb{R}^3$ and minimal surfaces in $\mathsf{S}^3$.

**Theorem 1** *If $M$ is a simply connected minimal surface in $\mathsf{S}^3$ with data $g, A$, then there exists a CMC surface $\tilde{M} \subset \mathbb{R}^3$ with*

$$\tilde{g} = g \quad \textit{and} \quad \tilde{A} = \mathrm{id} + R^{\pi/2} \circ A. \tag{3}$$

In place of (2) we now have

$$A = \begin{pmatrix} 0 & \kappa \\ \kappa & 0 \end{pmatrix} \quad \text{and} \quad \tilde{A} = \mathrm{id} + R^{\pi/2} \circ A = \begin{pmatrix} 1-\kappa & 0 \\ 0 & 1+\kappa \end{pmatrix} \tag{4}$$

and this shows that $\tilde{M}$ is a MC1 immersion.

We can make the same construction as in the minimal case, because $\gamma_i \subset \mathsf{S}^3$ is ambient geodesic, or a great circle arc, if and only if $\tilde{\gamma}_i \subset \mathbb{R}^3$ is a planar curvature arc. Again we integrate $1-\kappa$ resp. $\kappa$ along the boundary arcs to the total turn $\tilde{\tau}_i$ of the normal along an arc $\tilde{\gamma}_i$ of the MC1 patch and the total rotation $\rho_i$ along the spherical arc $\gamma_i$ of the respective minimal patch. This gives

$$|\gamma_i| - \tilde{\tau}_i = \rho_i \tag{5}$$

where $|\gamma_i|$ is the length of $\gamma_i$. Although the lengths in (5) make it more complicated we can find an $n-3$ parameter family of closed spherical polygons with great circle arcs as before. We take Morrey's solution $M$ to the Plateau problem for such a polygon and conjugate back to a branched MC1 surface $\tilde{M} \subset \mathbb{R}^3$.

We are usually interested in further properties of $\tilde{M}$. For instance if we rule out branch points at the vertices then the complete MC1 surface turns out to be smooth. Moreover we want to specify $\tau_i$ as a real number; but both $\tau_i$ and $\tau_i$ plus integer multiples of $2\pi$ give rise to the same polygon. The standard way to deal with these problems is to embed the spherical boundary polygon into the boundary of a mean convex set.

## 2.1 A $C^1$-description of conjugation

The description explained before is disadvantageous for numerical considerations since a number of different numerical algorithms must be applied successively – all incorporating additional numerical inaccuracies: The spherical surface $M$ is the result of an area minimization process, this surface has to be differentiated twice, and finally the obtained geometric data must be integrated to the MC1 surface $\tilde{M}$. The discrete algorithm is based on a $C^1$ description which in the smooth case requires only one differentiation and integration. This description can be given for both minimal and MC1 surfaces. For details see [OP].

For the minimal surface case let $\Omega$ be a Riemann surface and $F : \Omega \to \mathbb{R}^3$ be a minimal immersion of $\Omega$ with normal vector field $N$. Then the conjugate surface $\tilde{F} : \Omega \to \mathbb{R}^3$ is given by the differential system

$$\begin{aligned} d\tilde{F} &= dF \circ R^{\pi/2} \\ \tilde{N} &= N. \end{aligned}$$

In a similar way the conjugate MC1 surfaces can be obtained from a spherical minimal surface. Take the Lie group representation of $\mathsf{S}^3$ and identify $\mathsf{S}^3$ with

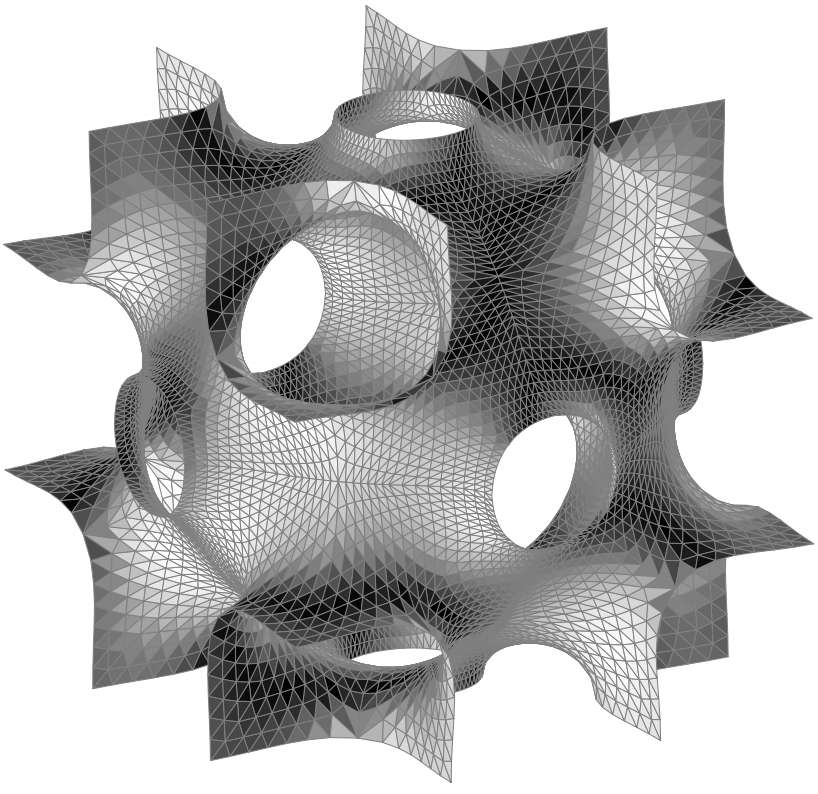

Figure 4: A translational fundamental domain of the triply periodic MC1 surface O,C-TO (we use A. Schoen's notation for a similar minimal surface). The domain is inscribed in a cube and has all its symmetries. The handle considered in the next figure sits in the middle of each face of the cube.

the unitary quaternions such that for $x \in \mathsf{S}^3$ we have $x = x_0 + x_1\mathbf{i} + x_2\mathbf{j} + x_3\mathbf{k}$. We identify $\mathbb{R}^3$ with the imaginary quaternions, $\operatorname{Im} x = (x_1, x_2, x_3)$. With $\bar{x} = x_0 - x_1\mathbf{i} - x_2\mathbf{j} - x_3\mathbf{k}$ the quaternion product is $\bar{x}y := (\langle x, y\rangle_{\mathbf{R}^4},\ x_0 \operatorname{Im} y - y_0 \operatorname{Im} x - \operatorname{Im} x \times \operatorname{Im} y)$.

**Lemma 2** *Let $F : \Omega \to \mathsf{S}^3$ be a minimal immersion, then the solution $\tilde{F} : \Omega \to \mathbb{R}^3$ of the differential system*

$$\begin{aligned} d\tilde{F} &= \operatorname{Im}(FdF \cdot R^{\pi/2}) \\ \tilde{N} &= \operatorname{Im}(FN) \end{aligned}$$

*is the conjugate MC1 surface in $\mathbb{R}^3$.*

## 2.2 The period problem

The period problem (compare Figures 4, 5) arises for compact MC1 surfaces except for the sphere. Suppose we want two planar symmetry arcs of a fundamental MC1 domain to be contained in the same plane. This is usually the case when an arc with total turn of the normal $\tilde{\tau}_i = \pm\pi$ is present. In general the $n-3$ parameter family of conjugate surfaces obtained from the spherical Plateau solutions leaves a nonzero translation, or *period*, between the two planes, and only a surface with a zero translation can generate a compact surface. If the periods can be closed at all, we expect that each period reduces the number of free parameters by one. The periods make our examples isolated (probably unique) in the class of surfaces we consider, i.e. with given symmetries: All examples in Section 5 have $n = 5$ boundary arcs and give rise to two period problems, whereas the Wente torus with $n = 4$ poses only one period problem.

In the easiest case of a one-parameter family the period problem is solved by an intermediate value argument [Ka] [G]: Two parameters with opposite periods are known, hence there is a surface with a vanishing period in between. Naturally, to apply the intermediate value theorem requires continuity of the surfaces in the parameter. This holds if the fundamental patch is a graph over a convex domain (see [Ka]). In [G] a different argument is applied to the Wente torus; a continuous family is selected by a mapping degree argument.

# 3 Numerical algorithm for discrete MC1 surfaces

Fundamental pieces of MC1 surfaces are rarely stable if they are considered as a solution to a free boundary value problem (cf. Section 4.2). Hence a direct numerical approach to the minimization of area under a volume constraint works only under very restrictive hypotheses, for instance for graphs in tetrahedra, see Anderson [ADNS]. Alternatively, integrals like $\int (H-1)^2$ could be minimized, e.g. using Brakke's evolver [Br].

Unlike the previous approaches the algorithm of Oberknapp and Polthier uses the technique of discrete geometric surfaces and discrete descriptions of their properties. Before, this was applied by Pinkall and Polthier [PP] to compute minimal surfaces and their conjugates. The discrete technique does not try to approximate the smooth problem as it is for instance the goal of the finite element theory. Instead it reformulates the problem on a discrete level and uses a

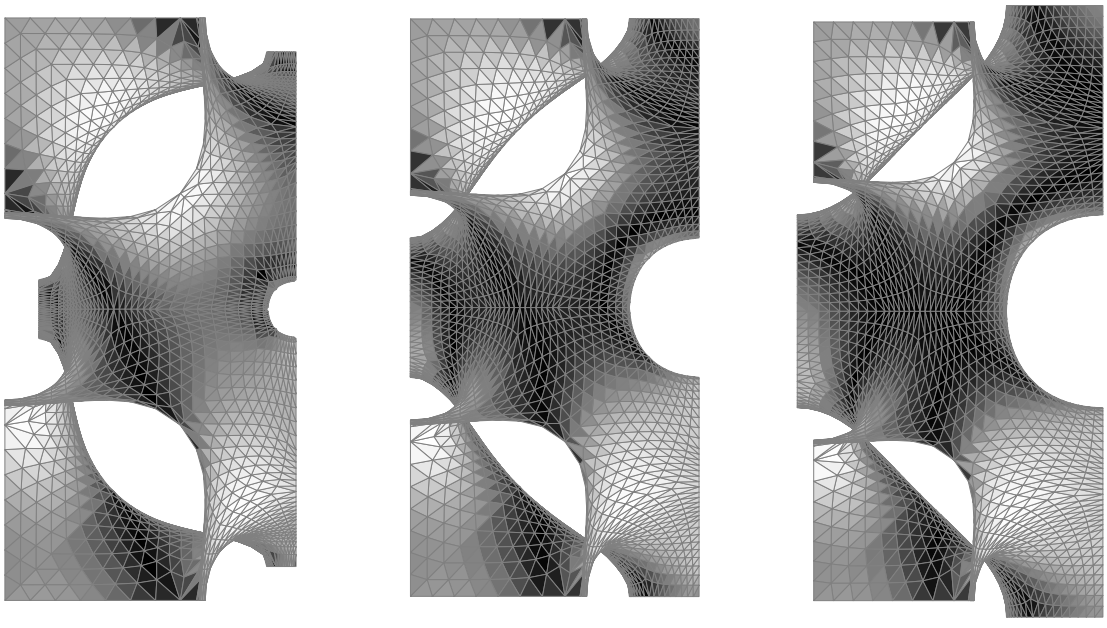

Figure 5: We demonstrate the period problem for O,C-TO. This surface can be generated by building an additional handle into the middle of each face of an I-WP MC1 surface. This handle on the left side of the first image is too small (negative period, say), correctly sized in the second image (0 period), and too big (positive period) on the last image.

description which is exact on this level. The advantage of the discrete approach comes from the fact that one tries to approximate a smooth situation only once, namely in the last step when the discretization goes to zero.

Let us review the algorithm of Oberknapp and Polthier. For a detailed description we refer to [O] [OP]. The algorithm consists of two parts. The first part is a method to compute the Plateau solution as a discrete minimal surface in $\mathsf{S}^3$. The second part consists of a conjugation procedure to compute the MC1 surface in euclidean space from the above Plateau solution. Before sketching the minimization part let us clarify some terms:

**Definition 3** (*i*) A *discrete surface in* $\mathsf{S}^3$ is a simplicial complex in $\mathbb{R}^4$ consisting of triangles whose vertices are restricted to $\mathsf{S}^3 \subset \mathbb{R}^4$; the triangles may degenerate to line segments or points. The surface is *discrete minimal* if variations of vertices constrained to $\mathsf{S}^3$ do not decrease the area of the simplicial complex in $\mathbb{R}^4$.
(*ii*) If two discrete surfaces $M_1$, $M_2$ have the same abstract triangulation then a *simplicial map* $f : M_1 \to M_2$ maps the corresponding vertices onto each other and is linear on each triangle.

For a simplicial map we define the Dirichlet energy by

$$E(f) = \frac{1}{2}\int_{M_1} |\nabla f|^2 = \frac{1}{4}\sum_{\text{edges } a_i} (\cot\alpha_i + \cot\beta_i)\,|a_i|^2\,,$$

where $|a_i|$ denotes the length of the edge on the image surface and $\alpha_i, \beta_i$ are the angles opposite to the edge $a_i$ in the two triangles containing $a_i$ in the domain. To obtain such a simple formula it is crucial to use linearity for the simplicial map in $\mathbb{R}^4$ rather than considering maps constrained to $S^3$. Starting with a discrete initial surface $M_0$ we define inductively simplicial surfaces $M_{k+1}$ to be the images of the minimum energy maps $f : M_k \to X$, where $X$ runs through all simplicial complexes with the correct boundary conditions. It can be shown that the sequence $M_k$ converges to a discrete minimal surface provided no triangles degenerate.

In $S^3$ the minimization routine needs an initial triangulation which is already quite dense. This is a result of the fact that the polygonal boundary in $\mathbb{R}^4$ of the triangulation does only approximate the geodesic boundary in $S^3$. For the surface an area defect results from the small caps between the triangulation in $\mathbb{R}^4$ and its projection to $S^3$. Now, if the triangulation is very coarse, then the defect becomes dominant. The effect which occurs is simliar to the following situation: When minimizing the area of a triangle with vertices restricted to a given cirle, then two vertices will move together. There are workarounds for this problem, but at the moment there is nothing known which works consistently with the conjugation algorithm other than our method above. This is an area of future research.

In a minimum $M$ the following equation is satisfied at every vertex $p$ of the triangulation

$$\frac{\partial}{\partial p}E(\mathrm{id})|_p = \frac{1}{2}\sum_{\substack{\text{vertices } q_i \\ \text{adjacent to } p}} (\cot\alpha_i + \cot\beta_i)\tan_p(p - q_i) = 0 \tag{6}$$

Here $\tan_p : T_p\mathbb{R}^4 \to T_p\mathsf{S}^3$ gives the tangential part of the vector $p - q_i$. This allows the discrete definition of conjugation. Geometrically (6) means that the weighted tangential parts of the edges emanating from $p$ in $M$ add up to zero. Hence they can be arranged as a closed polygon in the tangent space. This polygon is defined to be the dual cell at the point $p$ and can be understood as the integration of $*dF := dF \circ R^{\pi/2}$. Left translation moves the dual cell to the identity $T_{\mathrm{id}}\mathsf{S}^3$, where all cells are then reassembled (i.e. integration of the discrete data takes place) to a discrete MC1 surface in $\mathbb{R}^3$. If we take an $M_k$, $k \neq 0$, in place of the

minimum, conjugation is defined as above and the MC1 surface is approximated.

The complete numerical algorithm consists of the following steps:

- Read vertex angles and the total turning angles $\tilde{\tau}_i$ of the normal vector along each edge $\gamma_i$ of the fundamental patch for a euclidean MC1 candidate. Guess edge lengths $l_i$. Fix $n-3$ lengths and take the remaining three lengths as an initial condition for a rootfinder. By an adjustment of these three lengths the rootfinder generates a polygonal contour $\Gamma$ in $\mathsf{S}^3$ with the given vertex angles and rotation of normal equal to $\rho_i = l_i - \tilde{\tau}_i$.
- Solve the Plateau problem for $\Gamma$. In our examples the Gauß curvature varies considerably within a patch. Therefore interactive local refinement of the triangulation in regions of high curvature is necessary.
- The conjugation algorithm transforms a discrete minimal surface in $\mathsf{S}^3$ into a euclidean MC1 surface.
- Check periods of the resulting MC1 surface and repeat all steps with a different set of $n-3$ fixed initial lengths.

In practice we apply the algorithm to a one-parameter family of lengths at a time.

In principle, degeneracies can occur: The length of an edge can degenerate to 0 and also different arcs of the contour can intersect and give rise to two non-connected minimal patches which do not fulfill the original specification. Since the trigonometric formulae for the edge lengths are involved we use a numerical algorithm, a rootfinder, to compute the exact values. In practise we are 'far away' from these degeneracies.

# 4 Candidates and necessary conditions

Basically we follow Kapouleas' idea to obtain candidates of MC1 surfaces. We start with a *graph* with almost, but not exactly, integer edge lengths. In the simplest case the edge length is always close to 2. Our MC1 surfaces are close to spheres of radius 1 about the vertices of this graph. They are joint by handles whenever the respective vertices on the graph are joint by edges, and the graph is a topological retract of the MC1 surface. However, unlike Kapouleas, we do not admit scalings of the graph. Instead, for a given graph we check for existence

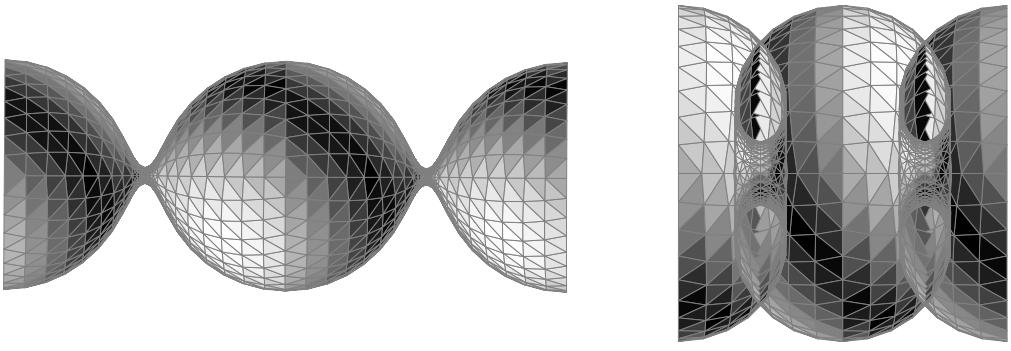

Figure 6: Delaunay surfaces: An embedded unduloid on the left, and on the right a nodoid cut open to display its self-intersections.

of the respective MC1 surface. There are necessary conditions for the graph and the types of handles we can use, that we want to describe in this section.

The prototypes of the handles we use are given by the Delaunay surfaces: We will construct *unduloidal handles* that look like those of the embedded unduloids, and, if small, resemble catenoids, and *nodoidal handles* that are close to the merely immersed nodoids (see Figure 6). Compared to a chain of spheres the period of the unduloids is bigger whereas the period of the nodoids is smaller. It is therefore reasonable to take unduloidal handles on the edges with length bigger than 2 and nodoidal handles on edges smaller than 2.

For the conjugate surface construction the type of handle we use is encoded in the data of the boundary polygon. A graph with planar symmetries and prescribed types of handles determines the vertex angles and total rotation of the boundary polygon, but not its lengths. In particular the two types of handles are distinguished by different values for the total turn of the normal $\tau_i$. This can be seen for the Delaunay surfaces: On the meridian of an unduloid the interior normal has 0 total turn from one sphere to another, or almost $+\pi$ in a neighbourhood of a small neck; on the meridian of a nodoid the total turn is $-2\pi$ between two spheres, or $-\pi$ in a neighbourhood of a small neck (cf. Figure 6). However different 'sizes' of the handles are not distinguished by a different turn of the normal but by a different weight, and therefore a different arc length, see the next subsection.

Kapouleas used these two types of handles. Other handles are possible, though: In [G] $n$ spheres are joint directly with each other. We believe these handles arise for compact MC1 surfaces too, see Figure 12 and 13. In this case the graph contains edges with length close to 1, and the trinoidal handle is placed

at the middle vertex .

## 4.1 The balancing formula

The balancing formula is due to Rob Kusner (see e.g. [KKMS, p.16ff]). To formulate the balancing formula we associate *weights* $w_i$ to each edge (or handle) of the underlying graph of a MC1 surface. For each handle this weight is determined as the integral of the conormal of a homological 1-cycle minus the integral over the normal of a homological 2-cycle which is bounded by the 1-cycle. Suppose the surface has a symmetry plane across a handle. We can take the 1-cycle $\gamma$ to be the planar curvature line in the symmetry plane winding once around a handle and bounding a disk $D$ in the symmetry plane. Then $w = \text{length}(\gamma) - 2\,\text{area}(D) > 0$ for an unduloidal handle and $w = -\text{length}(\gamma) - 2\,\text{area}(D) < 0$ for a nodoidal handle.

For each edge we let $e_i$ be the unit vector pointing away from the vertex in the direction of the edge and $w_i$ the weight of the corresponding handle. The balancing formula requires that the weighted directions sum up to zero,

$$\sum w_i e_i = 0, \tag{7}$$

with the sum running over all edges emanating from the vertex. For a given graph we can check that the distribution of unduloidal and nodoidal handles (reflected in lengths bigger and less than 2) is consistent with the balancing formula, i.e. we consider the signs in (7) only. In particular, if all vectors $e_i$ point into a half-space as they do on the outermost vertices of a compact MC1 surface, then there must be both positive and negative weights, or unduloidal and nodoidal handles. The precise weights are assigned to the edges by the numerical algorithm for a surface with zero periods. Hence (7) can be viewed as a necessary condition for the periods to close.

## 4.2 Stability

Stability imposes limits on the 'size' of a fundamental domain we can deal with: Since we use (both theoretically and numerically) the area minimizer to span a given spherical contour, we require that the spherical minimal patch $M$ is *stable* with respect to a fixed boundary. This means that the second variation of area of $M$ in $\mathsf{S}^3$ is non-negative, or

$$0 \leq \delta^2_{uN}\text{area}(M) = \int_M |\nabla u|^2 - \left(2 + |A|^2\right) u^2 \tag{8}$$

holds for all compactly supported $u$ (see e.g. [S]). On the other hand a MC1 surface is a critical point of the functional [area $- H$vol]. It is called *stable* if the second variation of this functional is non-negative, or

$$0 \leq \delta^2_{uN}(\text{area}(\tilde{M}) - H\text{vol}(\tilde{M})) = \int_{\tilde{M}} |\nabla u|^2 - |\tilde{A}|^2 u^2, \tag{9}$$

see e.g. [BdC, L.2.8]. Provided the boundaries are fixed the stability of the euclidean MC1 surface is equivalent to the stability of the conjugate minimal surface, that is: conjugation respects stability. We thank Rob Kusner who suggested the following lemma.

**Lemma 4** *Suppose $M \subset \mathsf{S}^3$ is a simply connected minimal surface and $\tilde{M} \subset \mathbb{R}^3$ is its conjugate MC1 surface. Then $M$ is stable if and only if its conjugate $\tilde{M}$ is stable.*

*Proof:* We compare (8) and (9). If $A = \left(\begin{smallmatrix} \lambda & \kappa \\ \kappa & -\lambda \end{smallmatrix}\right)$ then $|A|^2 = 2\lambda^2 + 2\kappa^2$. As in (4) we get for a conformal metric $\tilde{A} = \left(\begin{smallmatrix} 1-\kappa & \lambda \\ \lambda & 1+\kappa \end{smallmatrix}\right)$ and therefore $|\tilde{A}|^2 = 2 + 2\lambda^2 + 2\kappa^2 = 2 + |A|^2$. □

The notion of stability our construction yields for the MC1 patches seems to be weaker than the sense of stability that arises from considering the MC1 patches as critical points of area for fixed enclosed volume, and with boundary constrained to the symmetry planes. E.g. a quarter of an unduloid bubble (or of an entire unduloid) is stable for our construction, and this was necessary for us to compute Figure **??**; nevertheless a soap film experiment in a little cube cannot reproduce any unduloid patch except for the cylindrical one (or part of the degenerate sphere). Indeed it was shown in [A] that no unduloid patch is stable; for a discussion of different notions of MC1 stability see [G].

A hemisphere and any subset of it is stable, whereas any superset is not stable. Now our examples of MC1 surfaces are close to unions of spheres and stability persists over small deformations. In our examples the stability of the fundamental MC1 patches is not hard to believe (but not proved): the patches consist of a quarter bubble of an outer sphere as well as some spherical triangle on the central sphere (see e.g. Figure 8); for the icosahedral surface it is only a tenth of the outer bubble (Figure 11). In general we expect that we can obtain fundamental MC1 patches with no half-bubbles in a straightforward way with our algorithm; if there are half-bubbles we are on the edge, and for fundamental domains containing more than half-bubbles there we have no chance to construct them.

# 5 The examples and their numerics

To show how the conjugate surface method applies to compact surfaces we computed three examples. We explain the Penta surface of genus 5 in detail and will be more sketchy with the genus 30 and 3 surfaces.

The genus 5 surface Penta consists of 6 bubbles in fivefold symmetry, see Figure 1. Its graph looks like a Chrysler star. Suppose the radial edges have length slightly less than 2. Then the six unit spheres about the vertices relate as follows: Each outer sphere intersects the central sphere, but the outer spheres leave some space in between each other. Accordingly we place positive weights, i.e. unduloidal handles, on the pentagonal edges, and negative weights, i.e. nodoidal handles, on the spokes.

When the handle size of the fundamental MC1 patch tends to 0 (i.e. its parameters are on the $\delta$-axis in Figure 8) the fundamental patches degenerate: The fundamental spherical patch degenerates to a two-gon with angle $\pi/2$ and a spherical triangle with edge lengths $\pi/5$, $\pi/2$, $\pi/2$. The corresponding MC1 patches degenerate to two touching spherical patches, again a two-gon and a triangle; its periods are given by the deviation of the lengths of the underlying graph from 2.

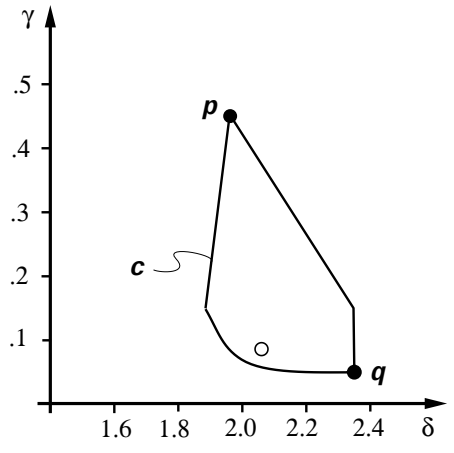


Figure 7: Numerical solution to the period problem for the Penta surface. The curve $c$ with winding number 1 contains the solution with zero periods (at the empty circle) in its interior. The curve is plotted in terms of the lengths of two curves of the closed boundary polygon, see the table above. The fundamental patch displaying the periods at the points $p$ and $q$ is given in Figure 8.

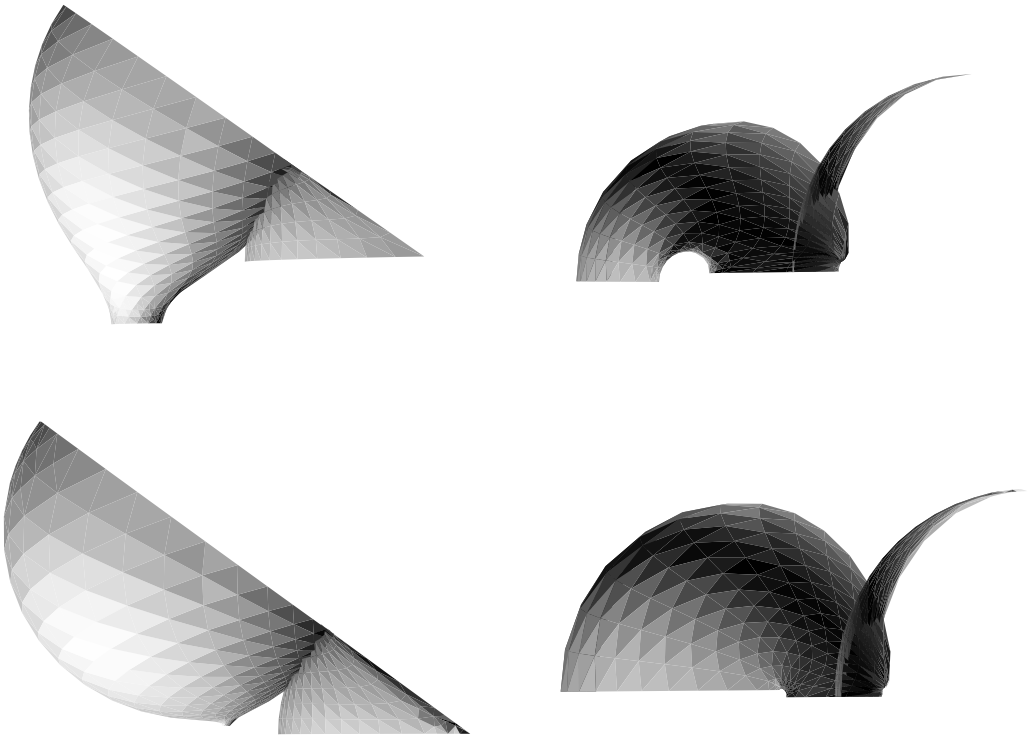

Figure 8: Fundamental domains of two Penta surfaces with non-vanishing periods. Top: Two different projections of the same fundamental domain at the point $p$ on the curve $c$, see Figure 7. The two different periods are given by the distance between the pairs of horizontal boundary lines in each projection. Bottom: Same for fundamental domain at $q$. At this point both periods have the other sign compared to $p$.

In the following table we summarize the data for the surface. The second row is the unduloidal handle curve, the last row the long curve containing the nodoidal meridian.

| arc (see Fig.7) | total turn of normal $\tau_i$ | edge angle at end of arc | length in degenerate patch | length of patch with closed periods |
|---|---|---|---|---|
| $\delta$ | $-\pi/5$ | $\pi/2$ | 2.20 | 2.05 |
| $\gamma$ | $-\pi$ | $\pi/2$ | 0 | 0.08 |
| | $\pi$ | $\pi/2$ | 1.57 | 1.72 |
| | $-\pi/2$ | $\pi/5$ | 1.57 | 1.63 |
| | $-5\pi/2$ | $\pi/2$ | 4.71 | 4.67 |

The periods give rise to a map $f$ from the two-dimensional moduli space of

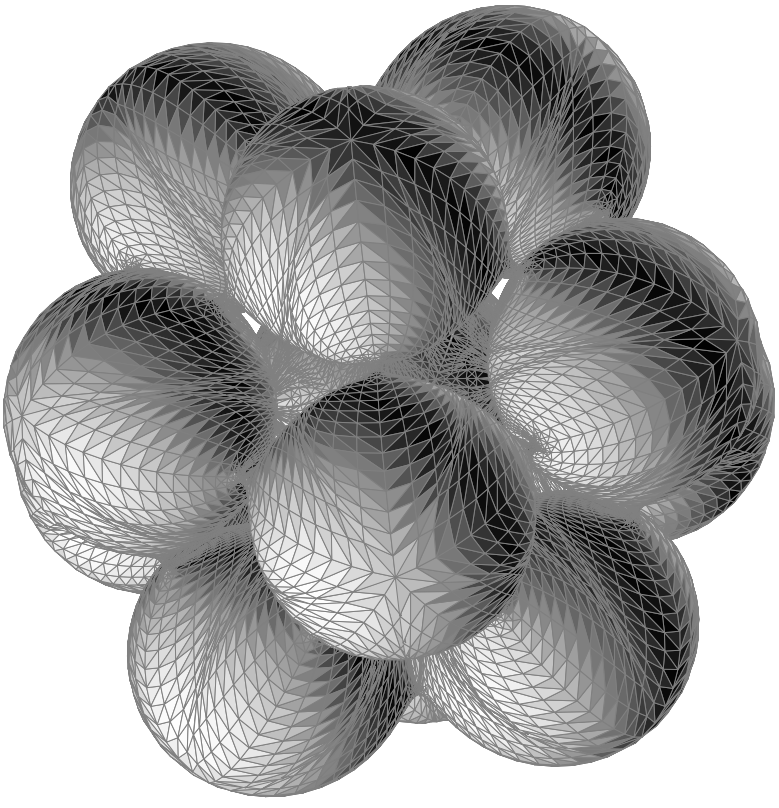

Figure 9: Surface of genus 30 with the symmetry of an icosahedron with unduloidal handles between the outer spheres and nodoidal handles joining each outer sphere with the centre sphere.

the Penta surface (with non-closed periods) into the two-dimensional space of periods. To locally parameterize the Penta surfaces we choose two lengths of the boundary polygon, namely those of $\gamma$ and $\delta$ in the table given above. We found a closed curve $c$ in the moduli space displayed in Figure 7 whose image under $f$ has winding number 1 around the origin in the period plane. The curve $c$ must enclose a surface with zero period which occurs at the parameter values corresponding to the empty circle in Figure 7. More specifically, on each of the four arcs on $c$ one period changes sign whereas the other period keeps its sign. Numerically, we computed the surfaces corresponding to the curve $c$. As an example we give the fundamental patch for two points $p, q$ on $c$ in Figure 8.

For the genus 30 surface the balanced graph is an icosahedron with one extra vertex in the midpoint and 12 more edges joining the midpoint to the vertices. Take these edges of length slightly less than 2 and consider unit spheres about each vertex as a starting surface. Then the centre sphere intersects the 12 outer

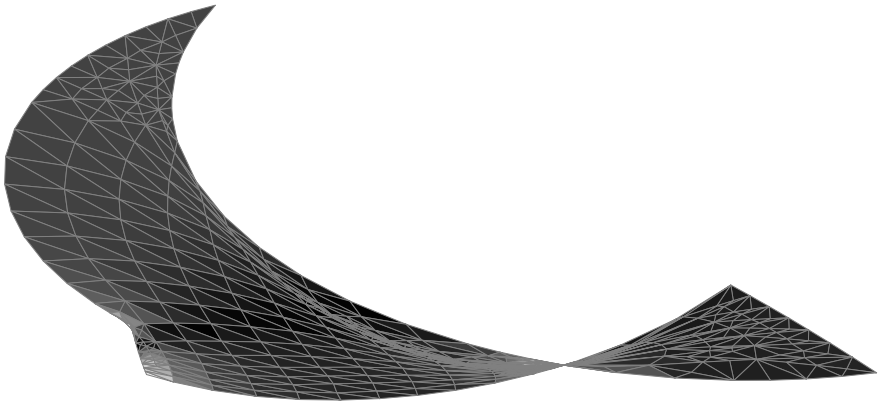

Figure 10: Fundamental domain for the icosahedral surface stereographically projected from $\mathsf{S}^3$ to $\mathbb{R}^3$. The small arc at the bottom left is the arc going half round the unduloidal handle, compare next figure. In the degenerate situation this arc has 0 length; the patch is then disconnected and conists of a two-gon with angle $\pi/5$ on the left and a spherical triangle on the right.

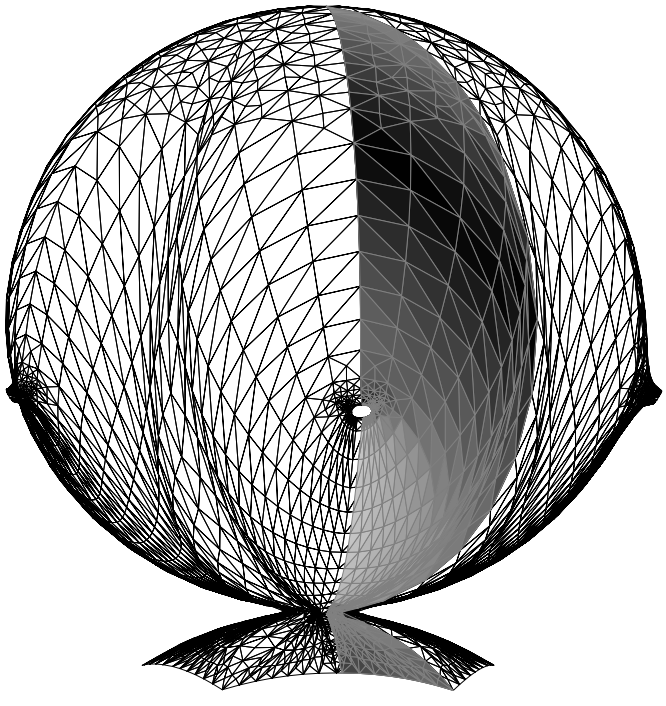

Figure 11: Icosahedral surface: One of the 12 outer bubbles that are attached to the centre-sphere with a nodoidal handle. A fundamental domain, conjugate to the spherical patch depicted in Figure 10 is highlighted.

spheres, but these spheres do not touch each other. This is obvious from the fact that in the less symmetric regular sphere packing each sphere touches 12 spheres. Hence in the most symmetric packing some space must be left in between the spheres. Accordingly we take nodoidal handles on the radial edges and unduloidal handles on the icosahedral edges. This surface was suggested by U. Abresch and is depicted in Figure 9.

The degenerate patch has two connected pieces: A spherical two-gon with angle $\pi/5$ (compare left hand side of Figure 10) and a spherical triangle with angles $\pi/2$, $\pi/5$, $\pi/3$ that is fundamental on $S^2$ for the symmetry group of the an icosahedron (see right hand side of the same figure). Again we summarize the data in a table. The table runs through the arcs in the anti-clockwise sense starting at the top left arc on Figure 10 or 11. The data in column 1 and 3 can be computed using trigonometric formulas.

| total turn of normal $\tau_i$ | edge angle at end of arc | length in degenerate patch | length of patch with closed periods |
|---|---|---|---|
| $-0.554$ | $\pi/2$ | 1.94 | 1.74 |
| $-\pi$ | $\pi/2$ | 0 | 0.10 |
| $-\pi$ | $\pi/2$ | 1.57 | 1.77 |
| $-0.365$ | $\pi/3$ | 0.55 | 0.36 |
| $-6.94$ | $\pi/5$ | 3.79 | 3.59 |

The underlying graph of the genus 3 surface is an equilateral triangle with three more edges from its midpoint to the triangle vertices. We take these spokes of length slightly bigger than 1. The degenerate surface consists of three spheres. These are joint by a trinoidal centre and nodoidal handles between each other. The numerical evidence for this surface is not conclusive: A small period remained, see Figure 14. In the forthcoming paper [GP] we discuss why it is reasonable, though, to believe that this surface exists.

# References


[A] Athenassenas, M.: A variational problem for constant mean curvature surfaces with free boundary, J. Reine und Ang. Math. **377**, 97-107 (1987)

[ADNS] Anderson, D.M., H.T. Davis, J.C.C. Nitsche, L.E. Scriven: Periodic surfaces of prescribed mean curvature Advances in chem. phys. **77**, New York: Wiley 1990

[BdC] Barbosa, J., M. do Carmo: Stability of hypersurfaces with constant mean curvature, Math. Zeit. **185**, 339-353 (1984).

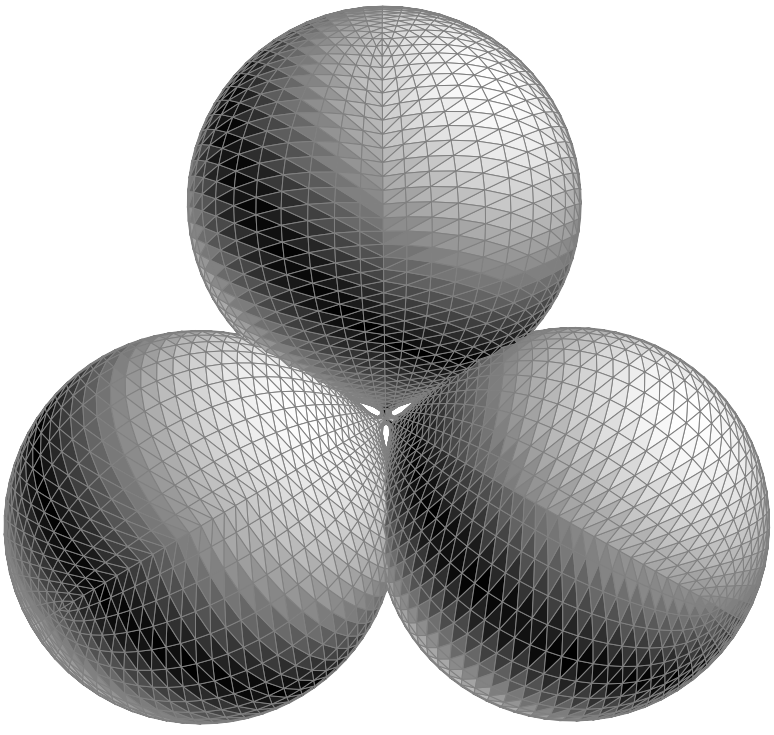

Figure 12: A genus 3 MC1 surface. The existence of this surface is not settled, since we did not achieve a complete closure of the period, see Figure 14 and Section 5.

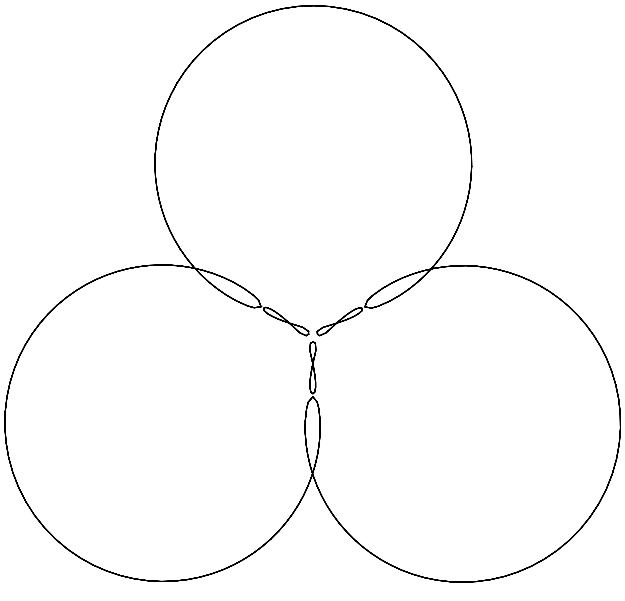

Figure 13: The intersection of the genus 3 surface with its symmetry plane displays the trinoidal handle in the centre and the nodoidal handles joining the bubbles pairwise.

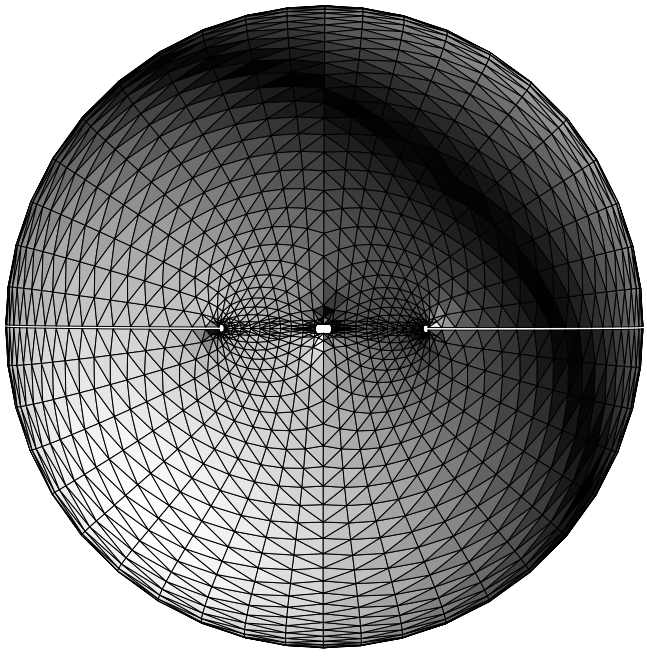

Figure 14: One bubble of the genus 3 MC1 surface displays the remaining period.


[Bo] Bobenko, A.I.: All constant mean curvature tori in $R^3$, $S^3$, $H^3$ in terms of theta functions, Math. Ann. **290**, 209-245 (1991)

[Br] Brakke, K.: The surface evolver, Exp. Math. **2**, 141-165 (1992)

[EKT] Ercolani, N., H. Knörrer, E. Trubowitz: Hyperelliptic curves that generate constant mean curvature tori in $\mathbb{R}^3$. The Verdier Memorial Conference on integrable systems, Actes du colloque international de Lumingy 1991.

[G] Große-Brauckmann, K.: New surfaces of constant mean curvature, Math. Zeit. **214**, 527-565 (1993)

[G] Große-Brauckmann, K.: A geometric existence proof for Wente-tori, preprint 1993

[G] Große-Brauckmann, K.: Stable constant mean curvature surfaces minimize area, to appear Pac. J. of Math. in 1997

[GP] Große-Brauckmann, K., K. Polthier: Numerical examples of compact constant mean curvature surfaces with low genus, in preparation.

[H] Heil, M.: PhD-thesis, TU Berlin, in preparation

[J] Jaggi, C.: On the classification of constant mean curvature tori in $\mathbb{R}^3$. Preprint ETH-Zürich, 1993.

[Ka] Karcher, H.: The triply periodic minimal surfaces of A. Schoen and their constant mean curvature companions. Man. Math. **64**, 291-357 (1989)

[Kp1] Kapouleas, N.: Compact constant mean curvature surfaces in euclidean three-space. J. Diff. Geom. **33**, 683-715 (1991)

[Kp2] Kapouleas, N.: Constant mean curvature surfaces constructed by fusing Wente tori. preprint

[KKMS] Korevaar, N., R. Kusner, W.H. Meeks, B. Solomon: Constant mean curvature surfaces in hyperbolic space, Am. J. Math. **114**, 1-43, (1992)

[L] Lawson, H.B.: Complete minimal surfaces in $\mathsf{S}^3$. Ann. of Math. **92**, 335-374 (1970)

[O] Oberknapp, B: Diplomarbeit Bonn, in preparation

[OP] Oberknapp, B., K. Polthier: A numerical algorithm for discrete surfaces with constant mean curvature, in preparation

[PP] Pinkall, U., K. Polthier: Computing discrete minimal surfaces and their conjugates, Exp. Math. **2**, 15-36 (1993)

[PS] Pinkall, U., I. Sterling: On the classification of constant mean curvature tori. Ann. of Math. **130**, 407-451 (1989)

[S] Schoen, R.: Estimates for stable minimal surfaces in three dimensional manifolds. In: Seminar on Minimal Submanifolds, Ann. of Math. Stud. **103**. Princeton: 1983

[W] Wente, H.: Counterexample to a conjecture of H. Hopf, Pac. J. of Math. **121**, 193-243, 1986

*Address of the authors*

Technische Universität Berlin
FB 3 Mathematik, MA 8-3
Str. des 17. Juni 136
10623 Berlin

kgb@sfb288.math.tu-berlin.de
polthier@math.tu-berlin.de